

Electrically directed assembly and detection of nanowire bridges in aqueous media

Robert J Hamers, Joseph D Beck, Mark A Eriksson, Bo Li,
Matthew S Marcus, Lu Shang, Jason Simmons and
Jeremy A Streifer

Department of Chemistry, University of Wisconsin-Madison, 1101 University Avenue,
Madison, WI 53706, USA

Received 16 January 2006

Published 19 May 2006

Online at stacks.iop.org/Nano/17/S280

Abstract

Although dielectrophoresis has been used previously to manipulate a variety of nanoscale materials, manipulation in ionic solutions is more difficult due to the high dielectric constant of water and the formation of electrical double-layers. Here, we report experiments aimed at the manipulation of nanowires in aqueous media and real-time detection of nanowire bridging events. Real-time video images demonstrate the ability to manipulate individual nanowires in aqueous media by capturing them along the edges of electrodes, and using a slow fluid flow to transport them until they bridge across micron-sized electrode gaps. By using special cancellation schemes, we demonstrate that it is possible to eliminate the effects of background currents through the electrolyte, and to electrically detect the bridging of electrodes by individual nanowires and nanowire bundles. These results have been obtained using gold nanowires with diameters ranging from ~50 to 250 nm, ~50 nm diameter silicon nanowires, and ~70 nm diameter carbon nanofibres.

 This article features online multimedia enhancements

(Some figures in this article are in colour only in the electronic version)

Although there are many examples of the assembly of individual nanoscale devices, the integration of multiple nanoscale components into complete systems remains challenging. This is particularly important in areas such as nanoscale sensing, where the ultimate goal is to fabricate and communicate with very large numbers of individually-addressable nanoscale sensors [1, 2]. To meet this challenge, it is necessary to develop the physical and chemical methods for assembly of nanoscale components that can be readily automated. One of the most attractive methods for fabricating devices is the use of dielectrophoresis. Dielectrophoretic manipulation has been used previously to assemble nanoscale circuits by bridging carbon nanotubes and inorganic nanowires across electrode gaps [3–12]. In the vast majority of cases, the manipulation has been performed in non-aqueous media because the high dielectric constant of water and the ubiquitous presence of ions limit the ability to perform dielectrophoresis.

Recently, there has been increasing interest in linking dielectrophoretic manipulation with the use of biomolecular recognition. For example, we reported the assembly and real-time electrical detection of individual metal nanowires that included biomolecular recognition between avidin and biotin to achieve more permanent assembly [12]. This work on gold nanowire assembly was a natural extension to previous work which used dielectrophoresis to manipulate individual bacterial cells across microelectrode junctions, with simultaneous measurement of the changes in electrical response when the bacterium bridged across the microelectrode junctions [13]. The ability to directly perform and observe the dielectrophoretic manipulation of individual nanowires in aqueous media has not been reported previously. The high dielectric constant, and the presence of ions in even relatively pure water make manipulation in aqueous media inherently more difficult than manipulation in common

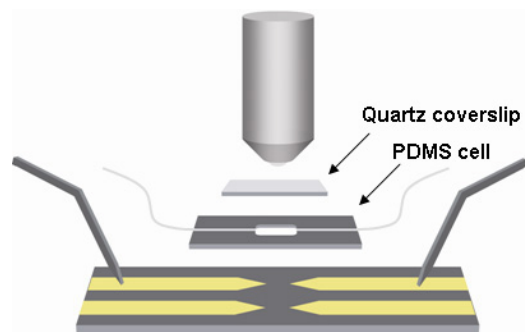


Figure 1. Schematic of fluid cell assembly for manipulating and detecting inorganic nanowires. A PDMS gasket creates a fluid channel above microfabricated electrodes, and is sealed with a quartz cover slip. The dynamic motion of the wires is imaged with an optical microscope, and electrical contact is made to the microelectrodes with electronic probes.

organic solvents. Yet, because most biomolecular recognition processes take place in ionic salt solutions, the combination of nanomanipulation with biomolecular recognition provides a motivation for developing the ability to manipulate and detect nanowire bridging processes in aqueous media.

Here, we report experiments aimed at the manipulation of nanowires in aqueous media and real-time detection of nanowire bridging events. We present real-time video images demonstrating the ability to manipulate individual nanowires in aqueous media. Furthermore, using special cancellation schemes, we are able to virtually eliminate the effects of background currents through the electrolyte, and still electrically detect the bridging of electrodes by individual nanowires and nanowire bundles. These results have been obtained using gold nanowires with diameters ranging from ~ 50 – 250 nm, ~ 50 nm diameter silicon nanowires, and ~ 70 nm diameter carbon nanofibres.

1. Real-time imaging of nanowire motion

In order to image and capture the dynamic motion of nanowires in real time, we constructed a probe station that integrates an optical microscope, electrical probes, and a microfluidic assembly. Figure 1 shows a schematic of a flow cell used for manipulation and detection of nanowires.

The microelectrodes used for dielectrophoretic manipulation and electrical detection are fabricated using a photolithographic process on a quartz or Si/SiO₂ substrate. Solutions containing nanowires are injected into a PDMS gasket that creates a fluid channel above the microelectrodes. The flow channel is sealed by clamping a thin glass cover slip on the top-side of the PDMS gasket. Metal probes are used to make electrical contact with the electrodes, and are connected to a voltage source used to create the electric fields necessary for dielectrophoretic manipulation. The electrodes and nanowire motion are imaged in real time with an optical microscope, and the image data are captured by software controlled CCD cameras.

Successful imaging of nanowires in solution requires careful attention to the optical path. Standard microscope objectives are optimized for imaging directly on the lower side of a quartz/glass cover slip. Successful imaging of

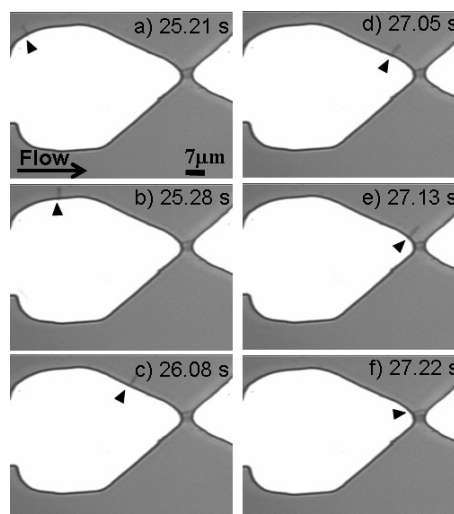


Figure 2. A series of still frame images from a video (supplementary information available at stacks.iop.org/Nano/17/S280) showing the manipulation of a silicon nanowire. The black arrows trace the trajectory of a single silicon nanowire as it is transported and assembled into a circuit element. The white 'tear-drops' are the metal electrodes, and the grey background is an insulator.

nanowire motion requires reducing optical distortion caused by long optical path lengths. The optical path length is minimized by using thin PDMS cells (1–2 mm) and thin quartz cover slips. We use either a low-magnification objective (10 \times) or a medium-magnification objective (40 \times) with an adjustable correction collar. In addition, images are usually obtained using a gelatin filter in the optical path to reduce chromatic aberration by restricting the range of wavelengths. The microscope objectives are also equipped with differential interference contrast as a method to further increase the contrast of the images.

Dielectrophoretic forces that are used for the manipulation of silicon nanowires, or any object, rely on inhomogeneous electric fields [14, 15] that are formed by applying an ac voltage across the electrode assemblies. Spatial variations in the electric field are a result of the large curvature at the edges of the individual electrodes (one energized, and one at ground). By combining the aligning ac potential with a continuous fluid flow in one direction, it is possible to use the hydrodynamic forces to gently push the nanowires along the edges of the electrodes and into the gap, essentially forming a simple nanowire transport system that assembles silicon nanowires into circuits. We originally demonstrated the ability to capture, transport, and detect individual bacterial cells. However, we have recently succeeded in applying this same method to achieve the controlled capture and transport of individual inorganic nanowires; this has been successfully achieved on three different types of nanowires: (1) silicon nanowires grown by the vapour–liquid–solid (VLS) mechanism [16, 17], (2) carbon nanofibres grown by plasma-enhanced chemical vapour deposition [18], and (3) gold nanowires fabricated by electrochemical deposition into an alumina or polycarbonate membrane [19, 20].

Figure 2 shows successive frames from a video showing the transport of a ~ 50 nm silicon nanowire along the edge of

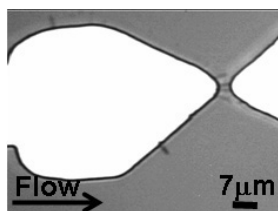


Figure 3. Wires are repelled from each other after the addition of another silicon wire.

the electrode and into a gap which is also occupied by several other nanowires previously captured via the same process. The complete movie showing the assembly of the silicon nanowire into an electrical circuit is available in compressed format as supplementary information at stacks.iop.org/Nano/17/S280. In this video the metal electrodes appear white, and the underlying silicon substrate appears grey. The nanowire is attracted to the electrode because of the dielectrophoretic force, and is transported along the electrode edge towards the electrode gap by the fluid flow (horizontal axis). The nanowire clearly follows the curving contours of the teardrop-shaped electrode and remains perpendicular to the edge of the electrode. Although in most cases it appears that one end of the nanowire is immediately adjacent to the electrode, in some cases a small amount of overlap is visible in which a nanowire may extend slightly over the top surface of the metallic electrode. As the nanowire progresses along the electrode surface, the nanowires captured at the electrode gap are clearly separated from one another, and remain approximately the same distance apart. The video shows that there is some faster motion of the nanowires which is probably a combination of Brownian motion and local turbulence due to the motion of the liquid around the electrodes.

As the nanowire enters the gap (figure 2(f)), the other nanowires slightly adjust their positions to accommodate this nanowire. One important observation from these studies is that the nanowires generally appear to repel one another. This can be clearly observed from images within the gap, and can also be observed along the electrode edges when higher densities of nanowires are used. A similar phenomenon was also observed in our previous measurements of bacterial cells where clear readjustments of position of bacteria along the electrode edges were observed. These repulsive interactions can have two origins: one from the possible presence of static charges on the nanowires [21], and the second is due to the polarization-induced dipoles that are formed in response to the alignment field; adjacent nanowires have their dipoles aligned along the same direction, and this dipole–dipole interaction leads to a repulsive interaction between adjacent nanowires.

Figure 3 shows a clear image of silicon nanowires trapped in an electrode gap by dielectrophoresis. The nanowires appear evenly spaced showing a balance between the dielectrophoretic force and a nanowire–nanowire repulsive force. The natural repulsion of the nanowires may be envisioned as a tool for creating self-assembled regularly spaced arrays of nanowires on an electrode. An understanding of the mechanism for nanowire–nanowire repulsion may allow for tunable array spacings and packing densities.

2. Manipulation of nanowires in ionic solutions

The dielectrophoretic manipulation of nanowires is based upon the ability to form inhomogeneous electric fields that extend from the electrodes into solution, as well as differences in the complex dielectric constant of the nanowire compared with the aqueous medium [14, 15]. The previous data demonstrating dielectrophoretic manipulation of silicon nanowires was performed in deionized water. In fact, most previous studies of nanowire manipulation have used deionized water or other dielectric fluids with negligible ionic concentration. However, in some circumstances the use of higher ionic strength media is desirable or even necessary. One important situation is where one desires to link nanoscale manipulation with the use of biomolecular recognition processes. Nanowires modified with biomolecules are able to recognize surfaces modified with complementary molecules. However, biomolecular recognition is often only effective in solutions whose composition approximates physiological conditions of approximately 0.1 M salt concentration. In the case of DNA hybridization, for example, the ions in solution screen the negative charges of the phosphate backbones so that the weak hydrogen bonds can form the DNA double helix. Although some biological systems can tolerate wide variations in salt concentration, many are only effective over a narrow range of conditions.

The manipulation of nanowires in ionic solutions is complicated by the formation of electrical double-layers at the junction of the electrodes and the solution. Ions in the double layer can effectively screen the charge on the electrodes, preventing the electric field from extending into the solution, and therefore hindering dielectrophoretic manipulation. The formation of the double layer creates a potential near planar electrodes of the form $\varphi \propto e^{-\lambda x}$ [22], where x is the distance from the electrode, and λ is the thickness of the double layer. For the static case the electric field is effectively confined to within the length scale of λ . The thickness of the electrical double-layer (λ) can be estimated based upon the well-known Gouy–Chapman theory as:

$$\lambda = \sqrt{\frac{\varepsilon \varepsilon_0 RT}{F^2 \sum_i c_i z_i^2}},$$

where ε is the dielectric constant of water (~ 78 near room temperature), ε_0 is the permittivity of free space, T is the temperature, F is the Faraday constant, c_i is the concentration of the i th ionic species (in mol m⁻³), and z_i is the ion charge (in multiples of the electron charge). For example, a 0.1 M solution of KCl has a double-layer thickness of approximately 1 nm, and in general, most ionic solutions have double-layer thicknesses close to this value. In virtually all solutions of interest, the double-layer thicknesses of ~ 1 –10 nm are small compared with the typical gaps (3–5 μ m typical values) between the electrodes. As the accumulation of ionic charge forms a double layer in response to the application of a potential, the electrical response of a double layer may be modelled as a capacitor. The complete electrical response of the electrodes in an ionic solution can be represented as a pair of capacitors representing the double-layer capacitance of each electrode, in series with a resistor representing the resistance of the solution. To a first approximation using Gouy–Chapman

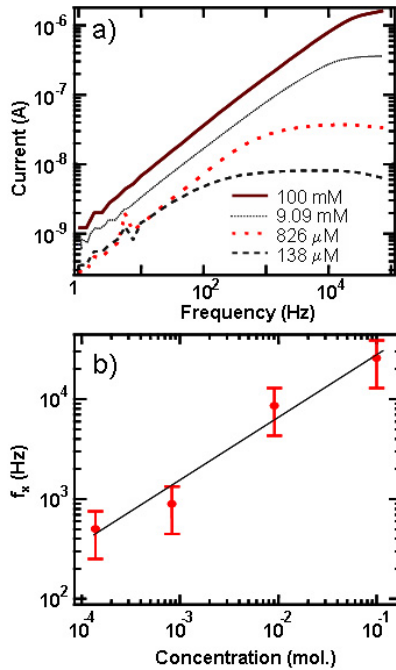


Figure 4. (a) Electrical response of the electrode–electrolyte circuit as a function of frequency and electrolyte concentration. (b) Cross-over frequency as a function of concentration.

theory [22], the capacitance per unit area of the double-layer is given by:

$$C = \sqrt{\frac{\varepsilon\varepsilon_0 F^2 \sum_i c_i z_i^2}{RT}} = \frac{\varepsilon\varepsilon_0}{\lambda},$$

and the resistivity (ρ), which is proportional to the solution resistance depends on the electrolyte concentration as:

$$\rho \propto \frac{1}{\sum_i \mu_i c_i z_i},$$

where μ is the ionic mobility. Although in reality the electrical response is complicated by a number of factors, including microscopic roughness of the electrodes and the complicated shapes of the electrodes, [23, 24] these equations are useful for qualitatively understanding the behaviour of the system.

The influence of the resistance and capacitance can be observed through measurements of the frequency-dependence of the current through the electrodes and its dependence on the concentration of ions in the electrolyte. Figure 4(a) shows the current versus frequency for different ionic concentrations using an excitation if $V_{\text{RMS}} = 10$ mV. For each electrolyte concentration, the plots show that the current increases approximately linearly with frequency at low frequencies, but then plateaus to a fixed value as the frequency increases beyond a critical value. The data at each electrolyte concentration can be easily modelled as a series combination of a resistor (the solution resistance) and two capacitors (the double-layer capacitance of each electrode). At low frequencies the impedance is dominated by the double-layer capacitance, and at high frequencies the solution resistance is dominant; the transition between the two regimes of behaviour then corresponds to a crossover frequency (f_x).

The low frequency data from figure 4(a) demonstrate log–log slopes less than unity, which deviate from approximating the double-layer with the Gouy–Chapman theory. To accommodate for the sub-linear slope, the double-layer is treated as a constant phase element (CPE). A CPE is a generalized capacitor that includes a non-integral dependence on frequency and the impedance is represented as: [24]

$$Z_{\text{cpe}} = \frac{1}{T(i\omega)^P}.$$

When the exponent P equals 1, then T is identically equal to the capacitance. For non-integral P , the interpretation of T is more complex and will not be discussed in more detail here [24].

The significance of the frequency-dependent data shown in (figure 4(a)) is that it demonstrates that at low frequencies the current is limited by the double-layer capacitance; in this case, the applied voltage is dropped primarily across the double-layers at the two electrodes, and there is very little voltage drop (and hence, only a small electric field) within the bulk liquid between the electrodes. In this situation, the dielectrophoretic force on the nanowires in solution is very small, and it is not possible to manipulate the nanowires. At higher frequencies where the current is independent of frequency, the overall current is limited by the resistance of the solution. In this situation, the ac modulation capacitively couples across the electrolytic double-layers and most of the applied voltage is dropped across the electrolyte solution, thereby resulting in a sufficiently large electric field within the bulk solution that can manipulate the nanowires. At each solution composition, it is straightforward to identify a crossover frequency, f_x , where the impedance of the CPE and of the resistor are equal, with dielectrophoretic manipulation facile at frequencies above f_x .

From an analysis of the data, it can be easily seen that as the ionic strength increases a higher frequency is required in order to manipulate the nanowires. This frequency-dependent relationship can be qualitatively identified using the simple Gouy–Chapman theory of the electrical double-layer [22]. The important feature to note is that while the solution resistance scales inversely with electrolyte concentration, the capacitance increases only with the square root of concentration. Consequently, the RC time constant, which separates the frequency ranges that are dominated by double-layer capacitance (at low frequencies) and by solution resistance (at high frequencies), is expected to increase with the square root of solution concentration.

Figure 4(b) shows a graph of the crossover frequencies (f_x) that were determined for four different concentrations of KCl. The values of f_x were found by first fitting the low frequency data from (figure 4(a)) to find the CPE parameters T and P , and then calculating the solution resistance (R_{sol}) from the plateau current values. Using the values for T , P and R_{sol} , the frequency f_x that satisfies $R_{\text{sol}} = Z_{\text{CPE}}$ was found. Fitting the log–log data to a line leads to a slope of 0.63, indicating that the crossover frequencies scales as $f_x \sim c^{0.63}$. This agrees well with the expected square-root dependence. The slight deviation probably arises from the fact that the simple theory is based upon plane-parallel electrodes with no microscopic roughness, whereas the complex shape of

our electrodes alters the behaviour somewhat. The significance of this concentration dependence is that it demonstrates that the electric field extends beyond the double layer and into solution at moderate frequencies ($f > 100$ kHz) such that it is feasible to achieve dielectrophoretic manipulation in solutions of ~ 0.1 M salt concentration.

The exact crossover frequency depends on the geometry of the electrodes but in general is within the range of easily accessible frequencies. Because at these frequencies the total impedance is small ($\sim 10^4 \Omega$ or less), it is also critical to ensure that the metal electrodes do not have significant impedance at the frequency of interest. In some electrode geometries we observe solution impedances comparable to the electrode resistance. When the electrodes and solution have comparable impedances a simple voltage divider is formed where a significant portion of the voltage is dropped along the length of the electrode instead of in the solution.

3. Electrical detection of gold nanowire bridging events

Although electric fields can clearly be used to manipulate nanowires, it is also possible to perform real-time measurements of the changes in electrical properties of the nanowire circuit. Most importantly, it is possible to directly detect the formation and destruction of nanowire bridges that form when a nanowire spans a gap between electrodes. The ability to detect bridging events as they occur is significant because it provides a simple pathway towards automated assembly of large numbers of nanowire bridges, using electrical signals both to create and to detect the bridges.

Electrical measurements of nanowire assembly are complicated by large background currents created by double-layer capacitances, low resistance electrolytes, and the high dielectric constant of water leads to very large stray capacitance at high frequencies. In fact, the background currents can easily be more than 1000 times higher than the change in current due to a nanowire bridging the gap between the electrodes. In order to be able to measure such small current changes we have used two different schemes for background current nulling.

In the first scheme (referred to as scheme 'a'), (figure 5(a)), two identical pairs of electrodes are used; each pair of electrodes consists of an 'excitation' electrode to which the ac modulation is applied, and a 'detection' electrode that is connected to the detection electronics. A small ac signal is directly applied to one excitation electrode and an inverted replica of this signal is applied to the second excitation electrode. The two detection electrodes are electrically connected together, and connected to a current-to-voltage converter. The amplified current is then read out by a computer controlled lock-in amplifier. If the two pairs of electrodes are geometrically identical, then the background currents through each pair of electrodes should be identical in magnitude but 180° out of phase, such that when the two signals are added they should cancel each other out before the amplification stage. Scheme 'a' has the advantage that it automatically compensates for time-dependent variations, such as variations in resistivity and dielectric properties of the electrolyte due to changes in concentration and/or temperature. However,

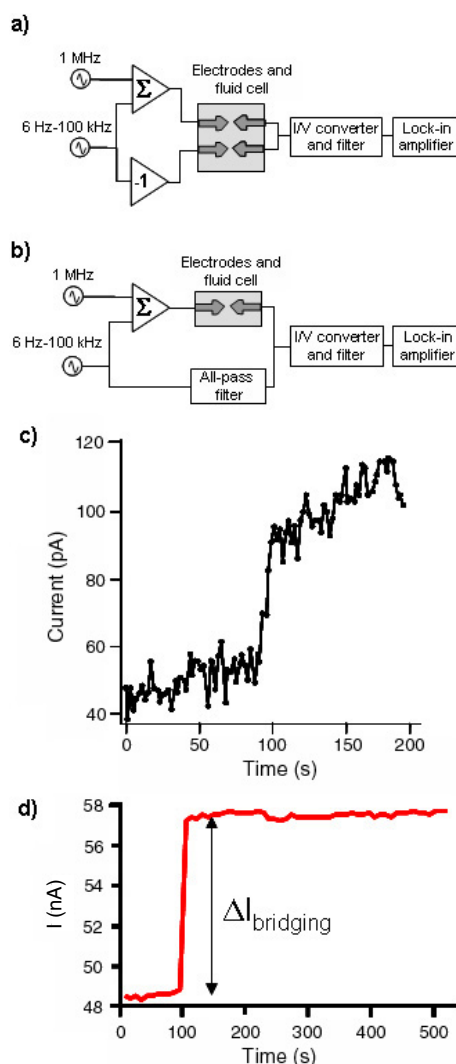


Figure 5. ((a), (b)) Different schemes for nulling background currents through solution. (c) Capacitive coupling causes a current increase of ~ 40 pA when a gold nanowire is manipulated into the electrode gap. (d) Current increase of ~ 10 nA when a gold wire functionalized with biotin binds to avidin-coated electrodes.

complete cancellation in this scheme is only effective if the two pairs of electrodes are geometrically identical.

In the second cancellation scheme (referred to as scheme 'b'), (figure 5(b)), only one pair of electrodes is used, and a phase-shifting circuit consisting of an 'all-pass' filter is used to create an inverted (i.e., 180° shifted) replica of the signal applied to the excitation electrode. This signal is additively coupled to the input to a current-to-voltage converter and summed with the current from the pair of electrodes being measured. By adjusting the amplitude and phase of the all-pass filter, it is possible to precisely null out all of the background current. In practice, we have found it possible to reduce the background current by $\sim 100\times$ using scheme 'b' alone.

Figure 5(c) shows one set of data that is typical of that which we observe using the all-pass filter (scheme 'b') to null out the background current. By nulling out the background current before the current-to-voltage converter, the experiment retains a high sensitivity. In this case, the background current

is almost completely removed, leaving only a small ~ 40 pA current which is due to imperfect cancellation. A slow upward drift in the current is observed and is most likely due to slow variations in temperature. Near $t = 100$ s, the bridging of a gold nanowire was observed visually with the microscope, and there is a very clear step-wise increase in the overall current. In general, the bridges formed by individual gold nanowires give rise to current changes of the order of 40–100 pA using a 10 mV excitation. Step-wise increases of this size have been observed for the bridging by individual nanowires, and decreases of this same magnitude have been observed when individual nanowires are released from the gap. Using the excitation voltage and the current change from a nanowire bridging event the associated impedance of a nanowire bridge is 100–250 M Ω .

The current change from a nanowire bridging the electrode gap ($\Delta I \sim 40$ – 100 pA) is at first surprising given that the gold nanowire is highly conductive with a conductivity estimated at ~ 1 S. Frequency-dependent impedance measurements of gold nanowires give insight into the dominant conduction mechanism for a nanowire bridges. Particularly, we find that the frequency-dependent impedance measurements indicate that a nanowire bridging event is dominated by a capacitive coupling [12]. The high impedance and frequency response of a nanowire bridge can be understood by approximating the nanowire as a cylindrical conductor above an infinite plane. The nanowire–electrode capacitance may be calculated with [25]¹

$$C_{\text{NW}} = \frac{2\pi\epsilon L}{\cosh^{-1}(2h/d)} \approx 6 \text{ fF},$$

where L is the nanowire–electrode overlap distance, h is the spacing between the electrode and the centre axis of the wire, and d is the diameter of the nanowire. Assuming the resistance of the nanowire is negligible compared to the capacitively coupled impedance, the current change from a wire bridging the gap is estimated at $\Delta I = \omega CV \approx 10$ pA (see footnote 1). Given the variation in nanowire–electrode overlap distance (L), as well as variations in the nanowire, diameters (d), and wire–electrode spacing (h), the estimate agrees well with data from the experiment.

In almost all cases the current change from a gold nanowire bridging across the electrode gap is of the order $\Delta I \sim 40$ – 100 pA. However, in some rare cases, the current increase can measure up to $\Delta I \sim 10$ nA. Figure 5(d) shows a real-time measurement of the current changing ~ 10 nA at $t = 100$ s. The current change corresponds to exactly when a gold nanowire is observed to bridge the gap with the optical microscope. We believe that bridging events that demonstrate large current changes (~ 10 nA) indicate that the nanowire has made a physical contact with the electrode, sometimes puncturing through biomolecular layers, whereas observed current changes of the order ~ 10 pA indicate a capacitive coupling.

It is interesting to note that an ohmic contact, where there is no significant contact resistance between the nanowire and the electrode, is *not* required to perform real-time electrical

detection of nanowires. The implication is that even with a large contact resistance, or where the nanowire is physically separated from the electrode, the presence of the wire is detectable. The capacitive detection becomes important in biosensing applications where 2–5 nm thick electrically resistive organic or biomolecular layers may coat both the electrode as well as the wire. Although the resistive organic layers may hinder dc conduction detection methods, we have demonstrated the ability to ac couple through the organic layers and detect the presence of a nanowire.

4. Extension to biomolecular recognition of chemically functionalized nanowires

Although dielectrophoretic manipulation represents one means for controlling the assembly of nanowires, the use of biomolecular recognition represents a complementary method that is more permanent and is based upon short-range chemical forces. Dielectrophoresis provides a temporary binding force for silicon and gold nanowires. When the manipulation field is turned off the silicon and gold nanowires tend to release from the electrodes as a result of the force from the fluid flow. Adding a local chemical force, such as a binding force provided by biomolecular recognition, allows the nanowires to be first positioned and then permanently attached to the electrodes.

Although there has been a great deal of work done on biomolecular recognition of small nanoparticles functionalized with biomolecules, comparatively little work has been done on the larger nanowire structures. In recent studies we found that the well-known interaction between avidin and biotin can be used to more permanently ligate nanowires in place after using dielectrophoretic manipulation [12]. Similarly, DNA hybridization can also be used such that nanowires of interest only interact with electrodes that are functionalized with DNA molecules having complementary sequences. These methods pave the way towards the fabrication of novel types of bio-electronic devices. However this is only feasible if the dielectrophoretic manipulation and detection can be performed in aqueous media, especially media containing salts at concentrations appropriate for the recognition processes to take place.

5. Summary

Dielectrophoretic forces can be used to manipulate a wide range of nanoscale materials and to create new types of nanoelectronic structures. The temporary assembly of nanowires into circuit elements using dielectrophoresis can be combined with the biomolecular recognition processes to achieve chemical selectivity, and to fabricate new types of sensing structures incorporating nanowires. We have demonstrated that it is possible to manipulate nanowires using dielectrophoretic forces in a variety of media, including salt solutions, and to directly detect nanowire bridging events electrically. The combination of electric field-directed assembly, electrical detection, and biomolecular recognition leaves open many possibilities for the creation of new types of nanoscale bio-electronic structures and devices.

¹ Parameters used for the estimates are nanowire diameter of $d = 250$ nm, wire separation of 10 nm, overlap length of $L = 500$ nm and dielectric constant of water. The excitation voltage for estimating the current is $V = 10$ mV at a frequency of 50 kHz.

Acknowledgments

This work was supported in part by the National Science Foundation Grant DMR 0425880 and DMR0210806 and the US Army Environmental Laboratory.

References

- [1] Jin S, Whang D, McAlpine M C, Friedman R S, Wu Y and Lieber C M 2004 Scalable interconnection and integration of nanowire devices without registration *Nano Lett.* **4** 915
- [2] Beckman R, Johnston-Halperin E, Luo Y, Green J E and Heath J R 2005 Bridging dimensions: demultiplexing ultrahigh-density nanowire circuits *Science* **310** 465
- [3] Duan X, Huang Y, Cui Y, Wang J and Lieber C M 2001 Indium phosphide nanowires as building blocks for nanoscale and optoelectronic devices *Nature* **409** 66
- [4] Nagahara L A, Amlani I, Lewenstein J and Tsui R K 2002 Directed placement of suspended carbon nanotubes for nanometer-scale assembly *Appl. Phys. Lett.* **80** 3826–8
- [5] Diehl M R, Yaliraki S N, Beckman R A, Barahona M and Heath J R 2002 Self-assembled, deterministic carbon nanotube wiring networks *Angew. Chem. Int. Edn* **42** 353–6
- [6] Smith P A, Nordquist C D, Jackson T N, Mayer T S, Martin B R, Mbindyo J and Mallouk T E 2000 Electric-field assisted assembly and alignment of metallic nanowires *Appl. Phys. Lett.* **77** 1399–401
- [7] Boote J J and Evans S D 2005 Dielectrophoretic manipulation and electrical characterization of gold nanowires *Nanotechnology* **16** 1500–5
- [8] Lu S, Chung J and Ruoff R S 2005 Controlled deposition of nanotubes on opposing electrodes *Nanotechnology* **16** 1765–70
- [9] Fan D L, Zhu F Q, Cammarata R C and Chien C L 2004 Manipulation of nanowires in suspension by ac electric fields *Appl. Phys. Lett.* **85** 4175–7
- [10] Dong L, Bush J, Chirayos V, Solanki R, Jiao J, Ono Y, Conley J F Jr and Uhlrich B D 2005 Dielectrophoretically controlled fabrication of single-crystal nickel silicide nanowire interconnects *Nano Lett.* **5** 2112
- [11] Chan R H M, Fung C K M and Li W J 2004 Rapid assembly of carbon nanotubes for nanosensing by dielectrophoretic force *Nanotechnology* **15** S672
- [12] Shang L, Clare T L, Eriksson M A, Marcus M S, Metz K M and Hamers R J 2005 Electrical characterization of nanowire bridges incorporating biomolecular recognition elements *Nanotechnology* **16** 2846
- [13] Beck J D, Shang L, Marcus M S and Hamers R J 2005 Manipulation and real-time electrical detection of individual bacterial cells at electrode junctions: a model for assembly of nanoscale biosystems *Nano Lett.* **5** 777
- [14] Jones T B 1995 *Electromechanics of Particles* (Cambridge: Cambridge University Press)
- [15] Pohl H A 1978 *Dielectrophoresis* (Cambridge: Cambridge University Press)
- [16] Wagner R S 1970 *VLS Mechanism of Crystal Growth Whisker Technology* (New York: Wiley–Interscience)
- [17] Wagner R S and Ellis C W 1964 Vapour–liquid–solid mechanism of single crystal growth *Appl. Phys. Lett.* **4** 89
- [18] Cruden B A, Cassell A M, Ye Q and Meyyappan M 2003 Reactor design considerations in the hot filament/direct current plasma synthesis of carbon nanofibres *J. Appl. Phys.* **94** 4070
- [19] Kovtikhova N I and Mallouk T E 2002 Nanowires as building blocks for self-assembling logic and memory circuits *Chem. Eur. J.* **8** 4355
- [20] Martin C R 1996 Membrane based synthesis of nanomaterials *Chem. Mater.* **8** 1739
- [21] Yang M, Neubauer C M and Jennings H M 1997 Interparticle potential and sedimentation behavior of cement suspensions: review and results from paste *Adv. Cem. Bas. Mater.* **5** 1
- [22] Bard A J and Faulkner L 2001 *Electrochemical Methods: Fundamentals and Applications* (New York: Wiley)
- [23] Mulder W M, Sluyters J H, Pajkossy T and Nyikos L 1990 Tafel current at fractal electrodes: connection with admittance spectra *J. Electroanal. Chem.* **285** 103–15
- [24] Macdonald J R and Kenan W R 1987 *Impedance Spectroscopy—Emphasizing Solid Materials and Systems* (New York: Wiley)
- [25] Ramo S, Whinnery J R and Duzer T V 1994 *Fields and Waves in Communication Electronics* (New York: Wiley)